Thermal Synthesis of Silver Nanoplates Revisited: A Modified Photochemical Process

Hongxia Yu,[†,‡] Qiao Zhang,[†,§] Hongyan Liu,[†] Michael Dahl,[†] Ji Bong Joo,[†] Na Li,[†] Lianjun Wang,[‡] and Yadong Yin*,[†]

[†]Department of Chemistry, University of California, Riverside, California 92521, United States, [‡]Jiangsu Key Laboratory of Chemical Pollution Control and Resource Reuse, School of Environmental and Biological Engineering, Nanjing University of Science and Technology, Nanjing 210094, China, and [§]Institute of Functional Nano& Soft Materials (FUNSOM), Soochow University, Suzhou, Jiangsu 215123, China. The manuscript was written through contributions of all authors.

ABSTRACT The well-known photochemical and thermal methods for silver nano-plate synthesis have been generally regarded as two parallel processes without strong connections. Here we report a surprising finding that both visible light and ambient O_2, which are critically important in the photochemical process, also play determining roles in the thermal synthesis. By designing a series of control experiments, we reveal that the typical thermal synthesis is essentially a modified photochemical synthesis coupled with the unique redox properties of H_2O_2. Light irradiation and dissolved O_2 are found to be essential for initiating the formation of nanoplates, but the continued growth of nanoplates is supported by the oxidative etching and subsequent reduction of Ag due to

H_2O_2. O_2 resulting from the catalytic decomposition of H_2O_2 etches small nanoparticles to produce Ag^+ ions, which are then reduced back to Ag^0 by anions of H_2O_2 to support the growth of nanoplate seeds. The involvement of H_2O_2 in the reaction significantly speeds up the nanoplate formation process. These findings not only greatly improve our understanding of the unique functions of H_2O_2 in the thermal synthesis, but also bridge the two well established synthesis processes with a unified mechanism, and significantly enhance the reproducibility of the thermal synthesis of Ag nanoplates by identifying the critical importance of ambient light and O_2.
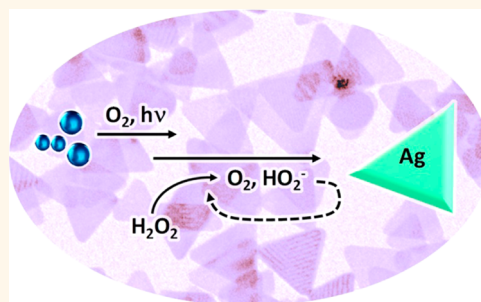
KEYWORDS: silver · nanoplates · photochemical synthesis · thermal synthesis · H_2O_2

Silver (Ag) has remained a model system for studying shape controlled synthesis of metallic nanocrystals due to its rich chemistry, in a role that CdSe has played in semiconductor nanostructure synthesis.[1−8] The standard reduction potential of silver in aqueous solution is 0.799 V, making its metallic form considerably stable but also easy to be attacked by strong oxidizing agents present in the surroundings. As a result, the colloidal synthesis of Ag nano-structures often involves not only the reduc-tion of Ag^+ but also the reoxidation of the metallic species, leading to very complex formation mechanisms and consequently low synthesis reproducibility.[9,10] The bene-fit of having these complex reaction path-ways, however, is the tremendous opportniu-ty for morphology control of Ag nanostruc-tures, as evidenced by the large variety of shapes demonstrated in literature.[3,11,12] Such architectural controllability, in combination with their strong size/shape-dependence of physiochemical properties, makes Ag nano-structures very attractive to researchers in many fields.[5−8,12,13]

Among the many types of Ag nanoparti-cles, nanoplates (also referred to as nano-prisms or nanodisks) represent a unique class of anisotropic structures that shows highly tunable plasmonic properties and promises great potential in many applications such as catalysis, sensing, and biomedicine.[14−17] Since the pioneering work on the photo-chemical synthesis of Ag nanoplates by Jin and Mirkin *et al.* in 2001,[2] a number of colloidal methods have been developed to produce such two-dimensional nanostruc-tures, including photochemical syntheses (also referred to as light-mediated methods) and thermal syntheses (also referred to as chemical reduction methods).[8] In a classic photochemical synthesis, plasmon exci-tation of preformed Ag nanoparticles by

visible light induces photochemical reactions that convert the small nanoparticles to larger nanoplates through the concurrent reduction of Ag^+ on the Ag particle surface and oxidative dissolution of small Ag particles by ambient O_2.[1,2,18−21] Light and O_2 have been found to be important factors in such syntheses, creating an effective ripening process that dissolves small unstable nanoparticles and promotes the growth of more stable nanoplate seeds.[19,20,22] On the other hand, typical thermal routes to produce Ag nanoplates follow a general formula: Ag^+ ions are reduced by a given reducing agent in the presence of one or more capping ligands to form Ag nanoparticles, which eventually evolve into plate shapes.[23−25] The most well-known high-yielding thermal synthesis was also initially developed by Mirkin et al., which involved the reduction of $AgNO_3$ with $NaBH_4$ in the presence of trisodium citrate (TSC), polyvinylpyrrolidone (PVP), and H_2O_2 at room temperature.[25] Although both ligands and $NaBH_4$ were found to impact the morphology of the products,[25−27] our systematic studies have revealed the critical role of H_2O_2 in the formation of silver nanoplates: it promotes the growth of nanoplates by removing less stable Ag nanoparticles of small sizes or other structures.[28,29] This understanding has allowed us to develop consistently reproducible processes for the synthesis of nanoplates with significantly improved efficiency and yields.[28,30]

The photochemical and thermal methods are generally regarded as two parallel processes without major overlap. In contrast to the extensively studied photochemical process,[18−20] the details of the thermal synthesis of Ag nanoplates have not been fully investigated and many important questions remain regarding the formation mechanism of the nanoplates. No studies have found any mechanistic connections between these two synthesis methods, even though both involve similar precursors, capping ligands, and reducing agents. Here we report a surprising finding that both visible light and ambient O_2, which are critically important in the photochemical process, also play determining roles in the thermal synthesis. Our systematic studies further reveal that the thermal synthesis is essentially a modified photochemical synthesis coupled with the unique redox chemistry of H_2O_2. The immediate significance of our results is the means to further enhance reproducibility of the thermal synthesis of Ag nanoplates: in addition to the appropriate synthesis recipes, one also needs to ensure sufficient exposure of the reaction system to visible light and ambient O_2. The results also significantly improve our understanding of the unique functions of H_2O_2 in the thermal synthesis. More importantly, our results bridge the two well established synthesis processes and provide a unified mechanism for the growth of Ag nanoplates in solution.

RESULTS AND DISCUSSION

A classic thermal synthesis of Ag nanoplates involves the reduction of an aqueous solution of $AgNO_3$ with $NaBH_4$ in the presence of TSC, PVP, and H_2O_2,[25,28] typically under air and magnetic stirring. In this reaction, $AgNO_3$ is the silver source, $NaBH_4$ is the reducing agent, citrate is the capping ligand that can selectively bind to the (111) facets of silver nanoparticles and thus help to maintain the plate morphology, PVP is a ligand that can improve the sample uniformity, and H_2O_2 has been previously identified as the key factor that defines the 2D plate symmetry of the products.[28] When performed, the reaction started with a light yellow color due to the formation of small Ag nanoparticles, turned to deep yellow after ~35 min, and then quickly changed to red, green, and blue within the next few seconds. The quick color transition at the later stage of the reaction was due to the plasmonic shift associated with the formation and growth of Ag nanoplates. The pH of the solution was ~9.0 initially and increased to ~9.7 near the end of the synthesis. As shown in Figure 1a, uniform Ag nanoplates with an edge length of about 40 nm could be successfully prepared by following the standard protocol described in the experimental section. The high yield of uniform silver nanoplates was further confirmed by the UV−vis spectrum (Figure 1b). The sharp peak around 650 nm and the weak shoulder around 420 nm can be assigned to the in-plane dipole and in-plane quadrupole plasmon resonance of Ag nanoplates, respectively. No sharp peak around 400 nm characteristic of spheres can be observed, confirming the high yield of silver nanoplates.

Although ambient O_2 has been found critical to the photochemical synthesis, its importance has rarely been recognized in thermal synthesis. In this work we designed a simple change to the standard reaction to reveal the surprising contribution of ambient O_2 to the thermal process. As shown in Figure 1c, when all the chemicals were first quickly mixed in a glass test tube under stirring and then allowed to sit without any further agitation, the reaction behavior changed dramatically (see also Video S1 in the Supporting Information). Consistent with the standard reaction, the initial solution was transparent and light yellow in color, suggesting the formation of very small Ag nanoparticles or clusters as the result of reduction of Ag^+ ions.[23,31] The Ag nanoparticles increased in size but maintained an overall spherical shape that resulted in a dark yellow solution after ~35 min. For convenience in later discussions, we define the nanoparticles at this stage as "quasi-spherical nanoparticles" according to their plasmonic band position, even though not all of them are strictly spheres. At ~ 35 min of the reaction, the air/liquid interface turned to deep blue, indicating the formation of anisotropic Ag nanoplates
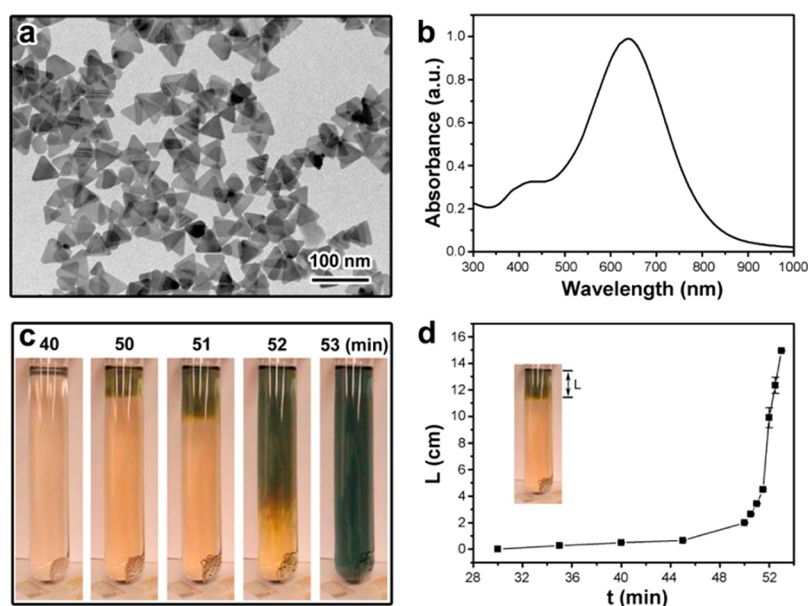
Figure 1. (a) A typical TEM image and (b) UV−vis absorption spectrum of silver nanoplates synthesized by the standard synthetic approach. In the absence of any agitation, (c) digital images showing the color change process; and (d) plot of the length of bluish solution as a function of reaction time.

at the interface. The deep blue region became highly discernible after 40 min, and kept expanding downward over time. The initiation and development of the blue region can be clearly seen in the digital images in Figure 1c. Meanwhile, bubbles were formed near the tube surface and rose from the bottom to the top. Interestingly, the color of the solution along the paths of the gas bubbles also changed to slightly bluish, implying that the gas bubbles can promote the formation of silver nanoplates. Figure 1d plots the change in length of the blue region as a function of reaction time, suggesting that the reaction progressed downward relatively slowly at the beginning and accelerated later.

The color propagation process from the top to the bottom is quite surprising because only homogeneous color change has been reported in thermal syntheses in literature.[25,28] As we observed in the reaction solution (Video S1, Supporting Information), the gas bubbles might be an important factor in the formation of silver nanoplates as the solution became blue when the bubbles formed. It is well-known that the decomposition of $NaBH_4$ and H_2O_2 can release H_2 and O_2, respectively. To investigate the composition of the gas bubbles as well as the growth mechanism, gas chromatography (GC) was used to study the reaction process in-depth. As shown in Figure 2a, both H_2 and O_2 can be detected during a standard reaction. At the beginning of the reaction, only H_2 could be detected and its amount decreased gradually, while no O_2 could be detected. Interestingly, when the solution became dark yellow, both oxygen and hydrogen concentrations spiked. The amounts of both oxygen and hydrogen rapidly reached their maxima within minutes and dropped to almost zero after another ∼30 min. Since

the dark yellow color indicated the formation of quasi-spherical silver nanoparticles, it is reasonable to suspect that the release of oxygen and hydrogen was triggered by these newly formed silver nanoparticles. To confirm this hypothesis, several control experiments were carried out.

When $AgNO_3$ was removed from the reaction system while the other parameters were controlled, no oxygen was detected within 60 min, as shown in Figure 2b. This result clearly rules out the possibility that H_2O_2 could decompose significantly after being exposed to ambient conditions for the designated period of time. Meanwhile, H_2 could still be detected in reduced amounts, but showed a release profile similar to that in the early stage of the standard synthesis, implying that $NaBH_4$ can decompose even in the absence of $AgNO_3$. Since in the original synthesis, the release of H_2 increased dramatically when the solution turned deep blue (Figure 2a), one would suspect either the quasi-spherical nanoparticles or nanoplates could promote the decomposition of $NaBH_4$. However, as shown in Figure 2c, when preformed silver nanoparticles or nanoplates were added to a mixture containing $NaBH_4$, TSC, and PVP, no significant change in the H_2 release profile was observed, implying that the metallic silver species were not able to dramatically promote the decomposition of $NaBH_4$. This fact is consistent with previous findings that metallic Ag is not a good catalyst toward the decomposition of $NaBH_4$ in aqueous solution.[32−34] One can therefore infer that the decomposition of $NaBH_4$ could be promoted by Ag^+ ions, which is, as discussed later, a reasonable conclusion that is consistent with additional experimental observations.
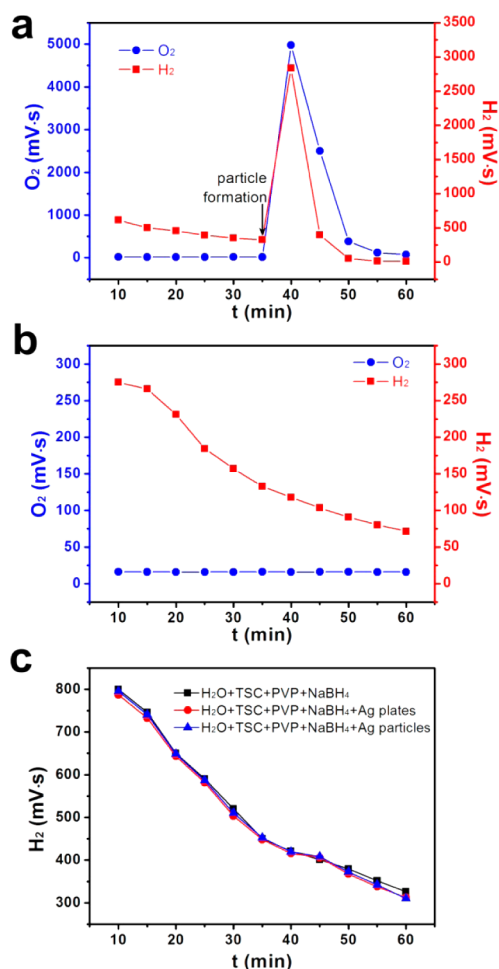
Figure 2. (a,b) The release of O_2 and H_2 as a function of the reaction time: (a) the standard synthetic approach; and (b) in the absence of AgNO$_3$. (c) The change of H_2 as a function of reaction time by replacing silver source with preformed Ag plates or particles.

Figure 3. (a) The release profiles of O_2 and H_2 in a typical synthesis but with H_2O_2 added after 490 min of reaction. (b) The corresponding UV−vis spectra of the solution collected at reaction times of 490 and 520 min.

Interestingly, there are no prior reports on the effect of Ag^+ on NaBH$_4$ decomposition, most likely due to the concurrent reduction reaction that always occurs when these two species are mixed.

Since both H_2 and O_2 were produced during the synthesis, one remaining question is whether or not H_2 gas plays a pivotal role in the formation of nanoplates. To investigate the role of H_2, we first made silver nanoparticles in the absence of H_2O_2 while controlling the other parameters. As shown in Figure 3a, a deep yellow solution was obtained after ~35 min and, as expected, only quasi-spherically shaped nanoparticles could be obtained from these conditions, as confirmed by the sharp peak at ~400 nm in the corresponding UV−vis spectrum (Figure 3b). The solution was further aged for several hours to allow complete depletion of the H_2 gas from the decomposition of NaBH$_4$, as shown in Figure 3a. Then a certain amount of H_2O_2 solution was quickly injected into the preformed nanoparticle solution. A rapid color change, from dark yellow to red, then green and ultimately blue, was observed,
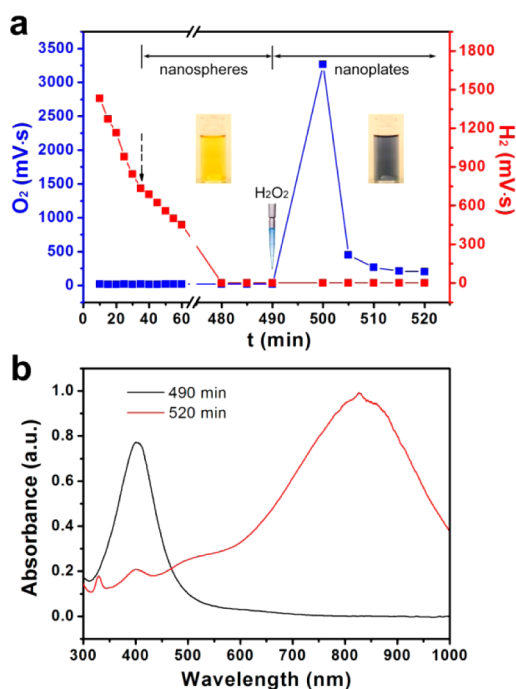
implying the conversion from quasi-spherical nanoparticles to anisotropic Ag nanoplates.[14,26,28] This conversion process was further confirmed by the UV−vis spectra shown in Figure 3b. Consistent with our previous observation, the formation of many gas bubbles was observed when H_2O_2 was injected. The GC test revealed that a large amount of oxygen had been produced, while almost no hydrogen could be detected (Figure 3a), further confirming the important role of H_2O_2 or its decomposition product O_2 gas. Another important conclusion is that the sudden release of O_2 is due to the decomposition of H_2O_2 by following the general reaction: $2H_2O_2 \rightarrow 2H_2O + O_2$. As NaBH$_4$ was completely depleted and no H_2 was released during the reaction, we can rule out the deterministic role of H_2 gas in inducing the formation of Ag nanoplates. However, an important question, which will be answered later, is what acts as the reducing agent to promote the nanoparticle-to-nanoplate transition.

By combining the new results with the observations in our prior studies,[28] we propose here a more comprehensive mechanism for the formation process of Ag nanoplates. At the early stage, Ag clusters or tiny nanoparticles were produced by the reduction of Ag^+ ions with NaBH$_4$ and stabilized by borohydride anions and citrate, as evidenced by the light yellow color of the solution.[28] A considerable amount of H_2 was released as promoted by Ag^+ ions, which were gradually converted into metallic species in the form of clusters and small nanoparticles. The reduction process

was balanced, however, by the oxidation of colloidal Ag by H_2O_2 without appreciable evolution of O_2 gas according to the following equations:[35]

$$Ag^0 + H_2O_2 \rightarrow Ag^+ + OH^- + \cdot OH \qquad (1)$$

$$Ag^0 + \cdot OH \rightarrow Ag^+ + OH^- \qquad (2)$$
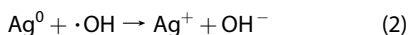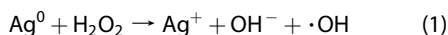
The competition between reduction by $NaBH_4$ and oxidation by H_2O_2 resulted in an overall low reduction rate, producing larger Ag nanoparticles after ~35 min of reaction. During this process, the decreased concentration of Ag^+ ions in the solution may partially contribute to the slower decomposition of $NaBH_4$ and consequently less release of H_2 gas (Figure 2a).

Although H_2O_2 is generally known as a strong oxidizer, it actually exhibits both oxidizing and reducing properties, depending on pH of the system. While H_2O_2 is indeed one of the most powerful oxidizers known in acidic solutions, it acts as a reducing agent and can reduce a variety of inorganic ions in basic solutions. Ekgasit et al. have observed that H_2O_2 can trigger the shape transformation of starch-stabilized Ag nanospheres to nanoplates without the involvement of additional reducing agents, and concluded that H_2O_2 functions as both a facet-selective etchant toward metallic Ag species and as a reducing agent toward Ag^+.[36] In the current case, due to the alkalinity of the solution, a large portion of H_2O_2 exists in the form of the anion HO_2^-, which has a standard reduction potential of 0.08 V.[37] When the size of the Ag nanoparticles reaches a critical value, the following reaction can take place to a considerable extent, so that Ag^0 and $HO_2\cdot$ radicals are produced according to the following equation:[35,38]

$$Ag^+ + HO_2^- \rightarrow Ag^0 + HO_2\cdot \qquad (3)$$
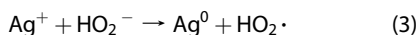
In an alkaline solution, the $HO_2\cdot$ radicals dissociate into their anion form O_2^-, which initiates the following chain reactions and leads to the rapid catalytic decomposition of H_2O_2 and consequently the burst release of O_2:[38]

$$O_2^- + H_2O_2 \rightarrow OH^- + \cdot OH + O_2 \qquad (4)$$

$$\cdot OH + H_2O_2 \rightarrow H_2O + HO_2\cdot \qquad (5)$$
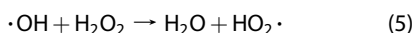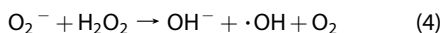
Oxidative etching has been recognized as a critical step in photochemical synthesis.[20] As reported by Xue and Mirkin et al., ambient O_2 was required for the transformation of the quasi-spherical Ag nanoparticles into Ag nanoplates. The major role of O_2 was to chemically convert the Ag nanoparticles into Ag^+, which was subsequently complexed by ligands and used as the Ag^+ source for the subsequent growth of nanoplates:

$$Ag^0 + 1/2 O_2 + H_2O \rightarrow Ag^+ + 2OH^- \qquad (6)$$
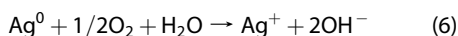
The concept of oxidative etching of metallic Ag by H_2O_2 has also been proposed in our previous studies of thermal synthesis.[28] Monitoring the colloidal solution

at the nanoparticle-to-nanoplate transition point using UV–vis spectrometry clearly showed that the intensity of the characteristic peak of quasi-spherical nanoparticles at ~400 nm quickly decreased, indicating their consumption due to oxidative etching. At the same time, another peak at ~500 nm emerged and gradually red-shifted to longer wavelengths, indicating the formation and growth of silver nanoplates. The role of H_2O_2 in the oxidative etching of Ag nanoparticles and promoting the growth of nanoplates was also subsequently confirmed by a number of other groups.[36,39] A general understanding now exists that the dissolution of Ag nanoparticles by oxidative etching supports the subsequent growth of Ag nanoplates by providing the needed Ag^+ source, which is a mechanism very similar to that proposed in photochemical reactions.

Now an interesting question arises: what is the ultimate oxidizing agent that etches the quasi-spherical Ag nanoparticles during the thermal synthesis, H_2O_2 (through eqs 1 and 2) or the large amount of O_2 resulting from the decomposition of H_2O_2 (through eq 6)? Another related question is if ambient O_2, which is the sole oxidizing agent in photochemical synthesis, could still contribute to the formation of Ag nanoplates in the thermal synthesis. To find clues to these questions, we conducted a series of experiments to carefully control the concentration of dissolved oxygen. As depicted in Figure 4a–c, we designed three setups with different conditions, named "ambient", "reduced O_2", and "low O_2", to study the influence of oxygen. In all cases, the initial concentrations of the reagents, including H_2O_2, were identical to those in the standard synthesis. For the "ambient" case, reactants were added directly into the deionized water, mixed well by brief stirring, and then kept unstirred under the ambient environment. For the other two cases, the reaction systems containing deionized water were first degassed by nitrogen bubbling for 2 h to minimize the dissolved O_2 content, then added reactants, stirred briefly ensure complete mixing, and finally exposed to ambient or N_2 atmospheres without stirring. The reaction system was maintained under nitrogen flow in the "low O_2" case, while it was exposed to ambient air in the "reduced O_2" case. While the concentrations of H_2O_2 and the other reagents were kept the same, the concentration of dissolved oxygen in the systems is believed to decrease in the order of "ambient" > "reduced O_2" > "low O_2". Although color could still be observed in all cases, the color change corresponding to nanoplate formation was not obvious in both the "reduced O_2" and "low O_2" cases. Ag nanoplates with considerably high yield were obtained in the "ambient" case, as confirmed by TEM imaging. The relatively lower quality of the products relative to that of the standard synthesis may be ascribed to the absence of agitation, which results in an inhomogeneous reaction system. Only about 50% yield of nanoplates was
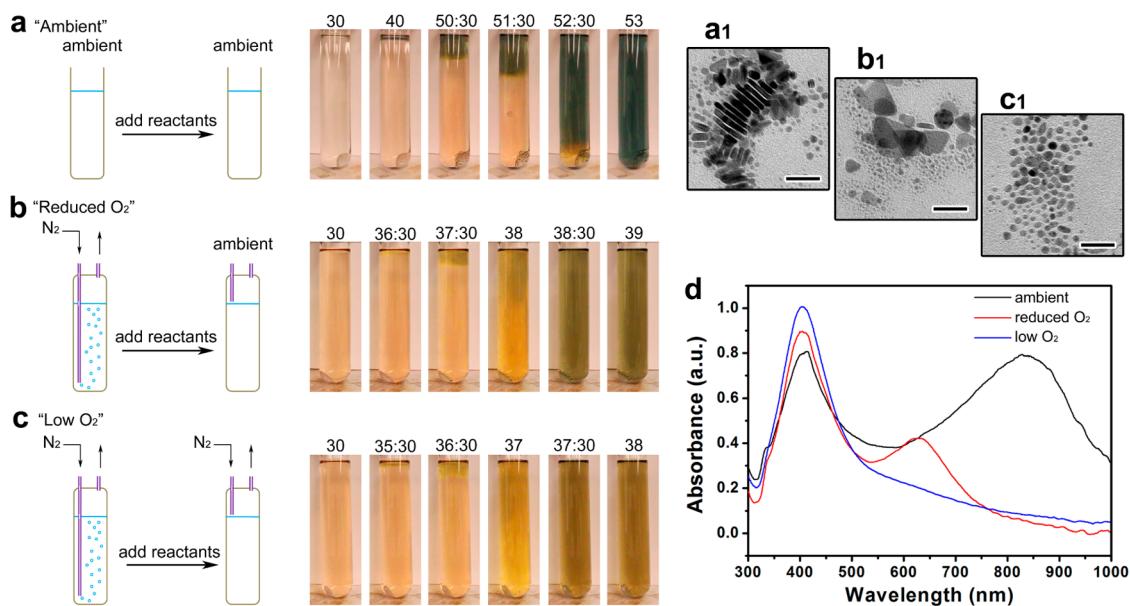
Figure 4. Schematic illustrations and digital images showing the formation of silver nanoparticles under (a) ambient, (b) reduced O_2, and (c) low O_2 conditions, along with corresponding TEM images (a_1, b_1, c_1) and UV−vis spectra (d) of the final products obtained after running reactions for 60 min. The scale bars are 30 nm.

achieved in the "reduced O_2" case; only small particles, including some plate-like ones, were obtained in the "low O_2" system. The results from TEM measurements were further confirmed by the UV−vis spectra, in which the peak in the long wavelength range could serve as an indicator for the yield of anisotropic structures. Careful observation indicated that in both the "ambient" and "reduced O_2" cases, nanoparticle formation initiated from the top surface of the solution and then progressed downward; this tendency was less obvious in the "low O_2" case. These control experiments clearly suggest the important role of ambient oxygen in the formation of Ag nanoplates. It should also be noted that the initial reduction rate seemed to be slower in the presence of dissolved oxygen, with the most significant delay occurring in the "ambient" case, indicating the counteracting effect of the dissolved oxygen against the reduction power of $NaBH_4$.

The above results seem to suggest that, in the thermal synthesis, H_2O_2 itself might not be the oxidizing agent that etches the quasi-spherical Ag nanoparticles (through eqs 1 and 2). The significant effect of the ambient O_2 on the reaction implies that the O_2 gas resulting from the decomposition of H_2O_2 may be the main player in the oxidative etching. This hypothesis, if valid, can explain the fact that nanoplates form only after the burst release of O_2 in the standard thermal synthesis. It is also consistent with the earlier observation that nanoplates could be seen forming along the pathway of the rising bubbles when the reaction was performed in test tubes without stirring. More importantly, it can explain the downward progression of the reaction front in the unstirred test tube (Figure 1c). The dissolved O_2, with the highest concentration at the

air/liquid interface, may initiate the oxidation of small quasi-spherical Ag nanoparticles and produce a sufficient amount of Ag^+ ions which are reduced and deposited onto the surface of more stable nanoplate seeds. The resulting large Ag nanoplates effectively catalyze the decomposition of H_2O_2 and produce a large amount of O_2 near the interface, and the resulting O_2 diffuses to nearby regions and further oxidizes the smaller and less stable quasi-spherical Ag nanoparticles below the interface. The chain reactions propagate downward until all the quasi-spherical silver nanoparticles in the test tube are converted to much larger and more stable nanoplates, which can survive against the oxidative etching by both H_2O_2 and O_2 due to their higher redox potentials.[18,31] As a considerable amount of ambient O_2 might be trapped on the tube surface during solution preparation, the reaction can also be initiated in lower regions near the tube surface and produce additional O_2 gas, which may combine with the H_2 resulting from the decomposition of $NaBH_4$ and produce large gas bubbles. These gas bubbles quickly rise to the surface, such that the formation of Ag nanoplates appears to start predominantly from the top surface of the solution. Such preferential initiation of the reaction cannot be observed in a standard synthesis, which is carried out under stirring so that ambient O_2 is dissolved uniformly throughout the solution. When the reaction is carried out under oxygen-free conditions, as shown in Figure 4c, the nanoparticle-to-nanoplate transformation cannot occur because in the absence of dissolved O_2, no substantial catalytic decomposition of H_2O_2 can be initiated.

A number of hypotheses have been proposed to account for the transition from silver nanoparticles to

nanoplates. In the photochemical synthesis, it is believed that dipole plasmon excitation may induce ultrafast charge separation on the nanoparticle surface, which leads to face-selective reduction of Ag^+ ions and anisotropic crystal growth.[8,18,20] This implies that any shaped seeds can be transformed into a nanoplate through dipole plasmon excitation, which is not fully consistent with the general understanding that the existence of (111) twin planes and stacking faults in seeds is required for them to grow into nanoplates.[40−45] In a different thermal reaction, Xiong and Xia *et al.* propose that slow reduction of Ag^+ ions may produce trimeric clusters of Ag that define preferential crystal growth into the plate shape.[46] We, along with others, believe that shape-selective oxidative etching holds the key to the dominant formation of nanoplates.[28,36,39,40] In the current thermal synthesis, we hypothesize that during the considerably long induction stage, due to H_2O_2 counteracting the reduction of Ag^+ by $NaBH_4$, many seeds containing (111) twin planes and stacking faults are formed. These nanoplate seeds are more stable against oxidative etching and they grow at the expense of less stable nanoparticles with smaller sizes and/or other shapes, which are dissolved by O_2 and serve as an Ag^+ source for nanoplate growth.

It is clear now that the function of H_2O_2 in the thermal synthesis is very similar to that of ambient O_2 in the photochemical synthesis, which is to provide Ag^+ ions, through oxidative etching of Ag nanoparticles, for subsequent nanoplate growth. An important question, however, remains: what reduces the dissolved Ag^+ ions back to Ag^0 atoms and deposits them on the growing Ag nanoplates? In Figure 3a, we demonstrated that Ag nanoplates can still be produced even after $NaBH_4$ has been completely depleted, so $NaBH_4$ is not necessarily the main reducing agent during the nanoparticle-to-nanoplate transformation. This conclusion was also recognized in a previous photochemical synthesis,[20] where it was proposed that the quasi-spherical Ag nanoparticles serve as photocatalysts that facilitate the reduction of Ag^+ ions onto their crystalline faces.[19,20,47] It was believed that the larger Ag particles could serve as seeds for nanoplates as well as photocatalysts for Ag^+ reduction by citrate and photoexcitation. Under light illumination, the plasmon excitation of the Ag nanoparticles produces hot electrons and holes, likely due to plasmon decay.[47,48] While the hot holes oxidize adsorbed citrate molecules, the hot electrons induce the reduction of Ag^+ ions onto the surfaces of the nanoparticles, leading to their growth into nanoplates.[19,20] This mechanism is consistent with the slow and light-intensity-dependent growth kinetics.

Since light plays an important role in the photochemical synthesis, we investigated if light irradiation has any effect on the formation of silver nanoplates in the
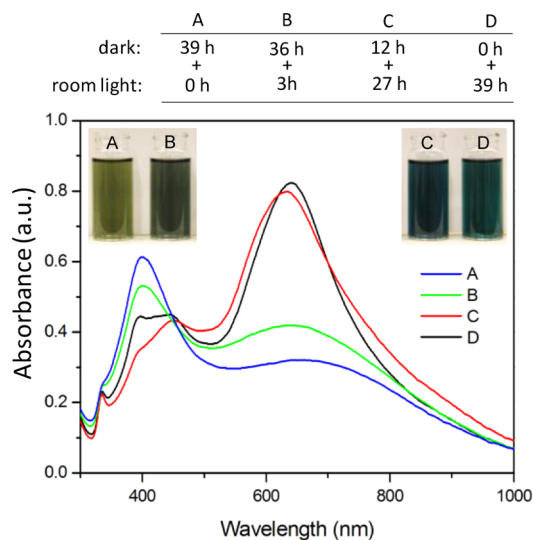

Figure 5. Digital photos of standard reaction solutions after being kept in the dark and then exposed to room light for various time periods. All the reactions were open to air. The total reaction time is 39 h for all samples.

thermal synthesis. We want to first point out that all the syntheses discussed so far were performed under room light irradiation. However, when a standard synthesis was carried out in dark, no nanoplates were formed. As shown in Figure 5, the solution remained yellowish green when it was kept in the dark for 39 h (Sample A). The corresponding extinction spectrum indicates the formation of mainly quasi-spherical nanoparticles with a small amount of anisotropic structures. When a solution was kept in the dark for 36 h and then brought into room light for another 3 h, the solution became dark green and the peak corresponding to nanoparticles decreased and the anisotropic peak increased (Sample B), suggesting the conversion to more nanoplates. A shorter aging time (12 h) and longer room light exposure (27 h) led to a deep blue color (Sample C) that is close to that of the sample prepared under room light for the entire 39 h (Sample D). suggesting the formation of mainly nanoplates, as confirmed by the dominant extinction peaks corresponding to the in-plane dipole plasmon resonance of nanoplates. We also observed that when the solution was aged in the dark first and then exposed to light, the nanoplate growth was slower, most likely due to the lower concentrations of $NaBH_4$ and H_2O_2 resulting from either decomposition or evaporation during aging. These results clearly demonstrate the importance of light in the transformation from nanoparticles to nanoplates in this standard thermal synthesis, which was previously not considered to be photochemically driven.

Understanding the critical need for light irradiation in the thermal synthesis makes us inclined to believe that light may play a role similar to that in the photochemical synthesis by promoting the nanoparticle-to-nanoplate transition through plasmon excitation. However, a major difference exists between these two
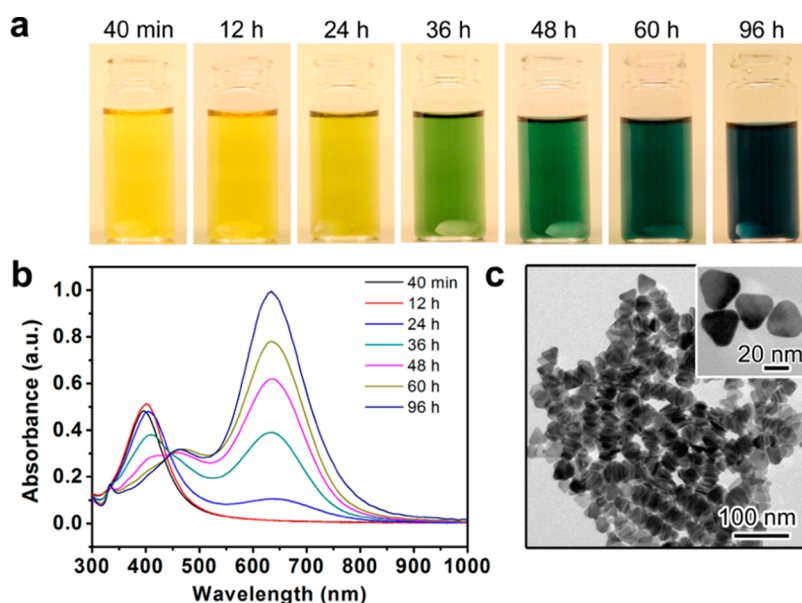
Figure 6. (a) Digital image and (b) UV−vis spectra showing the evolution process of silver nanoplate formation under the irradiation of laboratory ambient light; (c) TEM images of silver nanoplates prepared by this photoinduced method.

syntheses. In a typical photochemical synthesis, the particle-to-plate transition usually takes many hours to complete, even under strong light illumination, while in a standard thermal synthesis, it is extremely fast and completes within a few seconds. Thus, an additional reduction mechanism apparently exists, which we believe is caused by H_2O_2. As pointed out previously, H_2O_2 in an alkaline solution acts as a reducing agent that can reduce Ag^+ to Ag^0 through the reaction in eq 3. According to studies by Weiss and others, the catalytic reduction of Ag^+ by HO_2^- occurs in alkaline solutions only when colloidal silver particles grow to large sizes.[35,38] Likewise, in the current case, the nanoparticles are not catalytically active toward this reduction reaction until their growth into large nanoplates. This reduction reaction not only directly promotes nanoplate growth by depositing Ag^0 onto their surfaces, but also initiates the catalytic chain reactions of H_2O_2 decomposition eqs 4, 5 and releases O_2, which oxidizes small Ag nanoparticles into Ag^+ for supporting further nanoplate growth. In this case, light only serves as an "initiator" by producing a small amount of nanoplates, which then act as effective catalysts for the reduction of Ag^+ by HO_2^- through eq 3.

It is now clear that the thermal synthesis is in fact an interesting combination of a photochemical process with the unique redox properties of H_2O_2. Removing the H_2O_2 from this synthesis would lead to a photochemical synthesis which can still produce Ag nanoplates but much more slowly. To verify this understanding, we carried out another standard thermal synthesis but in the absence of H_2O_2, with the reaction system open to air and exposed to normal room light from a commercial fluorescent light bulb (with light intensity ~1500 lx). After ~40 min of

reaction, small silver nanoparticles formed, as supported by both the characteristic yellow color (Figure 6a) and the appearance of a sharp peak around 400 nm in the UV−vis spectrum (Figure 6b). After being irradiated for about 24 h, the solution color changed from yellow to slightly greenish, suggesting the evolution of nanoplates. After another 12 h of irradiation, the solution became green and a broad shoulder at ~650 nm appeared in the UV−vis spectrum, further confirming the formation of nanoplates. With a longer reaction time, the plasmon band of the Ag nanoparticles at 400 nm gradually disappeared and the characteristic band of nanoplates became more pronounced, implying the completed growth of silver nanoplates. As shown in Figure 6c, well-defined triangular silver nanoplates with almost 100% yield could be obtained after 96 h of light exposure. Light irradiation of higher intensity could dramatically speed up the reaction. When the light source was changed to a 250-W tungsten lamp with a light intensity of ~20000 lx, it took only 7 h instead of 36 h (in the case of room light) for the solution to turn green. Consistent with previous observations in the classic photochemical synthesis reported by Mirkin et al., we also found that no silver nanoplates could be obtained in the absence of either light or dissolved oxygen.[21] Compared to their process, the photochemical synthesis described here is much simpler, as it is a one step and one pot process without the need for the presynthesis of Ag nanoparticles. However, we believe the basic reactions involved in these two cases are actually very similar.

CONCLUSION

In summary, we have revealed that both visible light and ambient O_2, which are critically important in the

photochemical process, also play determining roles in the thermal synthesis of Ag nanoplates. Through a series of carefully designed control experiments, we show that the thermal synthesis is essentially a modified photochemical synthesis coupled with the unique redox properties of H_2O_2. The important factors that govern the photochemical synthesis such as light and dissolved O_2 still contribute to the formation of Ag nanoplates, but the catalytic decomposition of H_2O_2 and its reduction power in alkaline solution significantly speed up the nanoparticle-to-nanoplate transition. This is a surprising finding, as the well-known photochemical and thermal methods have been generally regarded as two different approaches for silver nanoplate synthesis. Our results should not only aid in enhancing the reproducibility of the thermal synthesis of Ag nanoplates by emphasizing the importance of ambient conditions, but also greatly improve our understanding of the unique functions of H_2O_2 in the thermal synthesis. Unifying the two well-established processes with a consistent mechanism also gives insight into the formation mechanism of other Ag nanostructures and helps in the design of new approaches for the synthesis of complex noble metal nanostructures in solution with high yields and reproducibility.

METHODS

Chemicals. Hydrogen peroxide (H_2O_2, 30 wt %) was purchased from Fisher Scientific. Silver nitrate ($AgNO_3$, 99+%), sodium borohydride ($NaBH_4$, 99%), sodium citrate tribasic dihydrate (TSC, 99%) were obtained from Sigma-Aldrich. Polyvinylpyrrolidone (PVP, MW $\approx$ 29 000) was purchased from Fluka. All chemicals were used as received without further treatment.

Synthesis of Silver Nanoplates. Thermal synthesis of silver nanoplates was carried out by following a previously reported procedure.[28] In a standard synthesis, a 24.75 mL aqueous solution combining $AgNO_3$ (0.05 M, 50 μL), TSC (75 mM, 0.5 mL), PVP (17.5 mM, 200 μL), and H_2O_2 (30 wt %, 60 μL) was stirred rapidly at room temperature in air, after which growth was initiated by rapidly injecting $NaBH_4$ (100 mM, 250 μL), immediately producing a light-yellow solution. In $\sim$35 min, the colloidal solution turned to deep yellow due to the formation of larger silver nanoparticles. Then the morphology started to change quickly from particles to nanoplates, accompanied by the solution color changing from deep yellow to red, green, and blue within the next several seconds.

Modifications were made to the standard synthesis for the purpose of revealing the contributions of various parameters. The specific changes to the standard procedure are described in the figure captions.

Characterization. The morphology of Ag nanoparticles was characterized by using a Tecnai T12 transmission electron microscope (TEM). Digital images and video were recorded with a Canon 50D digital camera. The measurement of optical property was conducted by using a probe-type Ocean Optics HR2000CG-UV-NIR spectrometer (190–1100 nm). The gases formed during the reactions were measured with a gas chromatograph (GC, HP-5890 Series II) equipped with a packed column (Molecular sieve 5A, Restek Corporation) which was connected to a thermal conductivity detector (TCD). The temperature of the oven was kept at 25 °C, and nitrogen was applied as a carrier gas with a column pressure of 20 psi. Typically, the gas outlet of the reactor was connected to the sample injector of the GC by a 6-way valve. The other carrier gas was continuously fed into the reactor at a flow rate of 5 mL min^{-1} and was mixed with the formed gas, then directed through the 6-port valve.

Conflict of Interest: The authors declare no competing financial interest.

Supporting Information Available: Video showing the preferential initiation of nanoplate formation at liquid/air interface. This material is available free of charge *via* the Internet at http://pubs.acs.org.

REFERENCES AND NOTES

1. Jin, R.; Charles Cao, Y.; Hao, E.; Metraux, G. S.; Schatz, G. C.; Mirkin, C. A. Controlling Anisotropic Nanoparticle Growth through Plasmon Excitation. *Nature* **2003**, *425*, 487–490.
2. Jin, R. C.; Cao, Y. W.; Mirkin, C. A.; Kelly, K. L.; Schatz, G. C.; Zheng, J. G. Photoinduced Conversion of Silver Nanospheres to Nanoprisms. *Science* **2001**, *294*, 1901–1903.
3. Xia, Y.; Xiong, Y. J.; Lim, B.; Skrabalak, S. E. Shape-Controlled Synthesis of Metal Nanocrystals: Simple Chemistry Meets Complex Physics? *Angew. Chem., Int. Ed.* **2009**, *48*, 60–103.
4. Xia, X.; Zeng, J.; Zhang, Q.; Moran, C. H.; Xia, Y. Recent Developments in Shape-Controlled Synthesis of Silver Nanocrystals. *J. Phys. Chem. C* **2012**, *116*, 21647–21656.
5. Sun, Y. G.; Wiederrecht, G. P. Surfactantless Synthesis of Silver Nanoplates and Their Application in SERS. *Small* **2007**, *3*, 1964–1975.
6. Tao, A. R.; Habas, S.; Yang, P. D. Shape Control of Colloidal Metal Nanocrystals. *Small* **2008**, *4*, 310–325.
7. Burda, C.; Chen, X. B.; Narayanan, R.; El-Sayed, M. A. Chemistry and Properties of Nanocrystals of Different Shapes. *Chem. Rev.* **2005**, *105*, 1025–1102.
8. Millstone, J. E.; Hurst, S. J.; Métraux, G. S.; Cutler, J. I.; Mirkin, C. A. Colloidal Gold and Silver Triangular Nanoprisms. *Small* **2009**, *5*, 646–664.
9. Xiong, Y.; Chen, J.; Wiley, B.; Xia, Y.; Aloni, S.; Yin, Y. Understanding the Role of Oxidative Etching in the Polyol Synthesis of Pd Nanoparticles with Uniform Shape and Size. *J. Am. Chem. Soc.* **2005**, *127*, 7332–7333.
10. Zheng, Y.; Zeng, J.; Ruditskiy, A.; Liu, M.; Xia, Y. Oxidative Etching and Its Role in Manipulating the Nucleation and Growth of Noble-Metal Nanocrystals. *Chem. Mater.* **2013**, *26*, 22–33.
11. Jones, M. R.; Osberg, K. D.; Macfarlane, R. J.; Langille, M. R.; Mirkin, C. A. Templated Techniques for the Synthesis and Assembly of Plasmonic Nanostructures. *Chem. Rev.* **2011**, *111*, 3736–3827.
12. Rycenga, M.; Cobley, C. M.; Zeng, J.; Li, W.; Moran, C. H.; Zhang, Q.; Qin, D.; Xia, Y. Controlling the Synthesis and Assembly of Silver Nanostructures for Plasmonic Applications. *Chem. Rev.* **2011**, *111*, 3669–3712.
13. Yin, Y.; Alivisatos, A. P. Colloidal Nanocrystal Synthesis and the Organic-Inorganic Interface. *Nature* **2005**, *437*, 664–670.
14. Zhang, Q.; Ge, J.; Pham, T.; Goebl, J.; Hu, Y.; Lu, Z.; Yin, Y. Reconstruction of Silver Nanoplates by UV Irradiation: Tailored Optical Properties and Enhanced Stability. *Angew. Chem., Int. Ed.* **2009**, *48*, 3516–3519.
15. Zeng, J.; Zheng, Y. Q.; Rycenga, M.; Tao, J.; Li, Z. Y.; Zhang, Q. A.; Zhu, Y. M.; Xia, Y. N. Controlling the Shapes of Silver Nanocrystals with Different Capping Agents. *J. Am. Chem. Soc.* **2010**, *132*, 8552–8553.
16. Sun, Y. G.; Xia, Y. N. Triangular Nanoplates of Silver: Synthesis, Characterization, and Use as Sacrificial Templates for Generating Triangular Nanorings of Gold. *Adv. Mater.* **2003**, *15*, 695–699.

17. Gao, C.; Lu, Z.; Liu, Y.; Zhang, Q.; Chi, M.; Cheng, Q.; Yin, Y. Highly Stable Silver Nanoplates for Surface Plasmon Resonance Biosensing. *Angew. Chem., Int. Ed.* **2012**, *51*, 5629–5633.

18. Maillard, M.; Huang, P.; Brus, L. Silver Nanodisk Growth by Surface Plasmon Enhanced Photoreduction of Adsorbed [Ag^+]. *Nano Lett.* **2003**, *3*, 1611–1615.

19. Wu, X.; Redmond, P. L.; Liu, H.; Chen, Y.; Steigerwald, M.; Brus, L. Photovoltage Mechanism for Room Light Conversion of Citrate Stabilized Silver Nanocrystal Seeds to Large Nanoprisms. *J. Am. Chem. Soc.* **2008**, *130*, 9500–9506.

20. Xue, C.; Métraux, G. S.; Millstone, J. E.; Mirkin, C. A. Mechanistic Study of Photomediated Triangular Silver Nanoprism Growth. *J. Am. Chem. Soc.* **2008**, *130*, 8337–8344.

21. Xue, C.; Millstone, J. E.; Li, S.; Mirkin, C. A. Plasmon-Driven Synthesis of Triangular Core—Shell Nanoprisms from Gold Seeds. *Angew. Chem., Int. Ed.* **2007**, *46*, 8436–8439.

22. Callegari, A.; Tonti, D.; Chergui, M. Photochemically Grown Silver Nanoparticles with Wavelength-Controlled Size and Shape. *Nano Lett.* **2003**, *3*, 1565–1568.

23. Murphy, C. J.; Gole, A. M.; Hunyadi, S. E.; Orendorff, C. J. One-Dimensional Colloidal Gold and Silver Nanostructures. *Inorg. Chem.* **2006**, *45*, 7544–7554.

24. Chen, S.; Carroll, D. L. Silver Nanoplates: Size Control in Two Dimensions and Formation Mechanisms. *J. Phys. Chem. B* **2004**, *108*, 5500–5506.

25. Metraux, G. S.; Mirkin, C. A. Rapid Thermal Synthesis of Silver Nanoprisms with Chemically Tailorable Thickness. *Adv. Mater.* **2005**, *17*, 412–415.

26. Zhang, Q.; Hu, Y.; Guo, S.; Goebl, J.; Yin, Y. Seeded Growth of Uniform Ag Nanoplates with High Aspect Ratio and Widely Tunable Surface Plasmon Bands. *Nano Lett.* **2010**, *10*, 5037–5042.

27. Zeng, J.; Tao, J.; Li, W.; Grant, J.; Zhu, Y.; Xia, Y. A Mechanistic Study on the Formation of Silver Nanoplates in the Presence of Silver Seeds and Citric Acid or Citrate Ions. *Chem.—Asian J.* **2011**, *6*, 376–379.

28. Zhang, Q.; Li, N.; Goebl, J.; Lu, Z.; Yin, Y. A Systematic Study of the Synthesis of Silver Nanoplates: Is Citrate a "Magic" Reagent? *J. Am. Chem. Soc.* **2011**, *133*, 18931–18939.

29. Li, N.; Zhang, Q.; Quinlivan, S.; Goebl, J.; Gan, Y.; Yin, Y. H_2O_2-Aided Seed-Mediated Synthesis of Silver Nanoplates with Improved Yield and Efficiency. *ChemPhysChem* **2012**, *13*, 2526–2530.

30. Liu, X.; Li, L.; Yang, Y.; Yin, Y.; Gao, C. One-Step Growth of Triangular Silver Nanoplates with Predictable Sizes on a Large Scale. *Nanoscale* **2014**, *6*, 4513–4516.

31. Henglein, A. Colloidal Silver Nanoparticles: Photochemical Preparation and Interaction with O_2, CCl_4, and Some Metal Ions. *Chem. Mater.* **1998**, *10*, 444–450.

32. Ma, J.; Choudhury, N. A.; Sahai, Y. A Comprehensive Review of Direct Borohydride Fuel Cells. *Renewable Sustainable Energy Rev.* **2010**, *14*, 183–199.

33. Chatenet, M.; Micoud, F.; Roche, I.; Chainet, E.; Vondrák, J. Kinetics of Sodium Borohydride Direct Oxidation and Oxygen Reduction in Sodium Hydroxide Electrolyte: Part II. O_2 Reduction. *Electrochim. Acta* **2006**, *51*, 5452–5458.

34. Hernández-Ramírez, V.; Alatorre-Ordaz, A.; Yépez-Murrieta, M. d. L.; Ibanez, J. G.; Ponce-de-León, C.; Walsh, F. C. Oxidation of the Borohydride Ion at Silver Nanoparticles on a Glassy Carbon Electrode (GCE) Using Pulsed Potential Techniques. *ECS Trans.* **2009**, *20*, 211–225.

35. Wiegel, E. The Mechanism of the Catalytic Decomposition of Hydrogen Peroxide on Colloid Silver. *Z. Phys. Chem., Abt. A* **1929**, *143*, 81–93.

36. Parnklang, T.; Lertvachirapaiboon, C.; Pienpinijtham, P.; Wongravee, K.; Thammacharoen, C.; Ekgasit, S. H_2O_2-Triggered Shape Transformation of Silver Nanospheres to Nanoprisms with Controllable Longitudinal Lspr Wavelengths. *RSC Adv.* **2013**, *3*, 12886–12894.

37. Atkins, P.; de Paula, J. *Physical Chemistry*, 7th ed.; W. H. Freeman: New York, 2001.

38. Weiss, J. The Catalytic Decomposition of Hydrogen Peroxide on Different Metals. *Trans. Faraday Soc.* **1935**, *31*, 1547–1557.

39. Tsuji, M.; Gomi, S.; Maeda, Y.; Matsunaga, M.; Hikino, S.; Uto, K.; Tsuji, T.; Kawazumi, H. Rapid Transformation from Spherical Nanoparticles, Nanorods, Cubes, or Bipyramids to Triangular Prisms of Silver with PVP, Citrate, and H_2O_2. *Langmuir* **2012**, *28*, 8845–8861.

40. Rocha, T. C. R.; Zanchet, D. Structural Defects and Their Role in the Growth of Ag Triangular Nanoplates. *J. Phys. Chem. C* **2007**, *111*, 6989–6993.

41. Lofton, C.; Sigmund, W. Mechanisms Controlling Crystal Habits of Gold and Silver Colloids. *Adv. Funct. Mater.* **2005**, *15*, 1197–1208.

42. Salzemann, C.; Urban, J.; Lisiecki, I.; Pileni, M. P. Characterization and Growth Process of Copper Nanodisks. *Adv. Funct. Mater.* **2005**, *15*, 1277–1284.

43. Goessens, C.; Schryvers, D.; Landuyt, J. V. Transmission Electron Microscopy Studies of (111) Twinned Silver Halide Microcrystals. *Microsc. Res. Technol.* **1998**, *42*, 85–99.

44. Germain, V.; Li, J.; Ingert, D.; Wang, Z. L.; Pileni, M. P. Stacking Faults in Formation of Silver Nanodisks. *J. Phys. Chem. B* **2003**, *107*, 8717–8720.

45. Elechiguerra, J. L.; Reyes-Gasga, J.; Yacaman, M. J. The Role of Twinning in Shape Evolution of Anisotropic Noble Metal Nanostructures. *J. Mater. Chem.* **2006**, *16*, 3906–3919.

46. Xiong, Y.; Washio, I.; Chen, J.; Sadilek, M.; Xia, Y. Trimeric Clusters of Silver in Aqueous $AgNO_3$ Solutions and Their Role as Nuclei in Forming Triangular Nanoplates of Silver. *Angew. Chem., Int. Ed.* **2007**, *46*, 4917–4921.

47. Redmond, P. L.; Brus, L. E. "Hot Electron" Photo-Charging and Electrochemical Discharge Kinetics of Silver Nanocrystals. *J. Phys. Chem. C* **2007**, *111*, 14849–14854.

48. Redmond, P. L.; Walter, E. C.; Brus, L. E. Photoinduced Thermal Copper Reduction onto Gold Nanocrystals under Potentiostatic Control. *J. Phys. Chem. B* **2006**, *110*, 25158–25162.